Breast Cancer Research

Breast Cancer RESEARCH

Phospho-ibuprofen (MDC-917) suppresses breast cancer growth: an effect controlled by the thioredoxin system

Breast Cancer Research 2012, **14**:R20 doi:10.1186/bcr3105

Yu Sun (yu.sun@stonybrook.edu)
Leahana M Rowehl (Leahana.Rowehl@stonybrook.edu)
Liqun Huang (liqun.huang@stonybrook.edu)
Gerardo G Machenzie (Gerardo.Mackenzie@stonybrook.edu)
Kvetoslava Vrankova (k.vrankova@googlemail.com)
Despina Komninou (desk@mediconinc.us)
Basil Rigas (basil.rigas@stonybrook.edu)

ISSN 1465-5411

Article type Research article

Submission date 2 September 2011

Acceptance date 31 January 2012

Publication date 31 January 2012

Article URL http://breast-cancer-research.com/content/14/1/R20

Phospho-ibuprofen (MDC-917) suppresses breast cancer growth: an effect controlled by the thioredoxin system

Yu Sun[1], Leahana M Rowehl[1], Liqun Huang[1], Gerardo G Mackenzie[1], Kvetoslava Vrankova[1], Despina Komninou[2], Basil Rigas[1, *]

[1] Division of Cancer Prevention, Department of Medicine, Stony Brook University, Stony Brook, New York, 11794-8173, USA;

[2] Medicon Pharmaceuticals, Inc, 18 Blueberry Ridge Rd, Setauket, NY 11733, Stony Brook, New York, 11733, USA

[*] **Corresponding author:** Basil.Rigas@stonybrook.edu

Abstract

Introduction

We have recently synthesized phospho-ibuprofen (MDC-917; P-I), a safer derivative of ibuprofen, which has shown anticancer activity. We investigated its efficacy and mechanism of action in the treatment of breast cancer in preclinical models.

Methods

We evaluated the anti-breast cancer efficacy of P-I alone or incorporated into liposomes (Lipo-P-I) in human ER (+) (MCF-7) and triple-negative (ER(-), PgR(-) and HER2(-); MDA-MB231) breast cancer cell lines, as they represent the most frequent (ER(+)) and the most difficult to treat (triple-negative) subtypes of breast cancer , and their xenografts in nude mice. We assessed the effect of P-I on a) the levels of reactive oxygen nitrogen species in response to P-I using molecular probes; b) the thioredoxin system (expression and redox status of thioredoxin-1 (Trx-1) and thioredoxin reductase activity); c) cyclooxygenase 2 (COX-2), nuclear factor κB (NF-κB) and mitogen-activated protein kinase (MAPK) cell signaling; and d) the growth of xenografts with stably knocked-down Trx-1.

Results

Compared to controls, a) P-I 400 mg/kg/day inhibited the growth of MDA-MB231 xenografts 266%; and b) P-I 300 mg/kg/day inhibited the growth of MCF-7 xenografts 51% and Lipo-P-I at the same dose 181%. In both cell lines, P-I induced oxidative stress and suppressed the Trx system (oxidized Trx-1 and decreased its expression; inhibited thioredoxin reductase activity). These changes triggered downstream redox signaling: the activity of NF-κB was suppressed and the Trx-1-ASK1 complex was dissociated, activating the p38 and JNK MAPK cascades. Trx-1 knockdown abrogated P-I's anticancer effect *in vitro* and *in vivo*.

Conclusions

P-I is safe and effective against breast cancer. Liposomal formulation enhances its efficacy; its effect is heavily dependent on the induction of oxidative stress and the suppression of the thioredoxin system. P-I merits further evaluation as an agent for the treatment of breast cancer.

Introduction

Breast cancer is the most frequently diagnosed cancer and the leading cause of cancer death among females owing, to a large extent, to the lack of effective and safe agents [1]. Phospho-ibuprofen (P-I, MDC-917) is a novel derivative of ibuprofen with significant efficacy against colon cancer and a favorable safety profile [2, 3]. Our preliminary data indicated that P-I might be effective in the treatment of breast cancer. Given the need for new agents for the control of breast cancer, we undertook a systematic study of the effect of P-I in breast cancer.

Thioredoxin (Trx), thioredoxin reductase (TrxR), and nicotinamide adenine dinucleotide phosphate (NADPH) comprise the thioredoxin system, which is crucial to redox homeostasis [4-7]. The Trx-1 isoform of Trx, the main intracellular antioxidant oxidoreductase [8-10], is normally in its reduced state (Trx-1-$(SH)_2$), defined primarily by two vicinal cysteine thiol groups at its active site (Cys32 and Cys35). When one of its client cellular proteins is oxidized, Trx-1-$(SH)_2$ reduces them, while "paying the price" of becoming itself oxidized in the process(Trx-1-S_2) . Normally, Trx-1-S_2 is rapidly restored to its functional reduced status (Trx-1-$(SH)_2$) by TrxR and NADPH.

The role of Trx-1 in breast cancer is not completely understood. Oxidative stress and activation of redox signaling pathways accompany breast cancer carcinogenesis and are correlated with prognosis in breast cancer patients [11]. As a rapid response molecule to oxidative stress, Trx-1 modulates redox signaling pathways via thiol-disulfide exchange with redox-responsive molecules, such as the transcription factors Ref-1 and NF-κB [9, 12, 13]; MAP3K5/ASK1 [14]; and the Trx-1 interacting protein (TXNIP) [10, 15]. The end result of these effects is modulation of cell kinetics, which sometimes, as we demonstrate here, can culminate in inhibition of cell growth and/or induction of apoptosis.. Another, recently appreciated consequence of oxidative stress is the induction of endoplasmic reticulum stress (ER stress) wich links it to inflammation with significant implications for several disorders including cancer [16, 17].

The level of Trx-1 is, overexpressed in human breast carcinoma compared to normal breast tissue and has been associated with breast cancer progression [18]. Furthermore, overexpression of Trx-1 or TrxR has been related to resistance to chemotherapy [19]. All these findings underscore the crucial role of the Trx system in breast cancer and establish it as a target for drug development [5, 20, 21].Here, we report the strong efficacy of P-I against breast cancer and establish the critical role of the thioredoxin system in mediating its anti-cancer effect through changes in downstream redox-responsive signaling pathways.

Materials and methods

Liposome-P-I (Lipo-P-I)

Lipo-P-I was generated following standard procedures by Encapsula NanoSciences LLC (Nashville, TN). The formulation is L-alpha-phosphatidylcholine (80 mg/ml), PEG-2000-DSPE (14.8 mg/ml) and P-I (45 mg/ml). The particle size is 200nm. The concentration of liposomal P-I was determined by HPLC before use [2].

Cell culture and cell viability and cytokinetic assays

We used MCF-7 and MDA-MB231 human breast carcinoma cell lines which reflect, to a large extent, the major features of cancer cells *in vivo* [22]. Estrogen receptor (ER) positive MCF-7 cells are human breast epithelial adenocarcinoma cells derived from the metastatic pleural effusion of a breast adenocarcinoma patient. This cell line retains several characteristics of differentiated mammary epithelium including the ability to process estradiol via cytoplasmic estrogen receptors and the capability of forming domes [23]. Triple negative (ER(-), PgR(-) and HER2(-)) MDA-MB-231 cells were obtained from a pleural effusion from a patient who had developed a 'poorly-differentiated tumor tending toward papillary configuration and tubule formation', while also having an intra-ductal carcinoma [24]. These cell lines were grown as recommended by the American Type Culture Collection (Manassas, VA), seeded at 5×10^4 cells/cm^2 for 24 h and then treated as indicated. We determined as previously described [25]: a) cell viability by the MTT assay (Roche Diagnostics); b) apoptosis by flow cytometry following staining with annexin V-FITC/ propidium iodide; c) cell cycle after staining with propidium iodide; and d) cell proliferation by the bromodeoxyuridine method.

Determination of Reactive Oxygen Nitrogen Species (RONS)

We assayed the following, as previously described [25]: a) *RONS* using the general probe dichlorofluorescine diacetate (DCFDA); b) *superoxide anion* (O_2^-) in whole cells by staining with 5 μM dihydroethidium (DHE) and analyzing fluorescence by flow cytometry, and c) *mitochondrial* O_2^- by seeding cells in glass bottom culture dishes, staining with MitoSOX™ Red and examining them under a Zeiss LSM510 confocal microscope.

Thioredoxin redox status assay

After each treatment, 10^6cells were lysed in 6 M guanidinium chloride, 50 mM Tris/HCl, pH 8.3, 3 mM EDTA, 0.5% Triton X-100 containing 50 mM iodoacetic acid [26]. After 30 min at 37°C, excess iodoacetic acid was removed using Microspin G-25 columns (GE Healthcare Life Sciences). Oxidized and reduced Trx-1 were separated by native PAGE, electroblotted onto a nitrocellulose membrane and probed with anti-Trx-1 antibody.

TrxR activity

TrxR activity was determined in the protein lysate using a commercially available kit, as per the instructions of the manufacturer (Cayman Chemical). In this assay, TrxR uses NADPH to reduce 5,5-dithiobis-(2-nitrobenzoic acid) to 5-thio-2-nitrobenzoic acid (TNB).

Immunoblotting and Electrophoretic Mobility Shift Assay (EMSA)

After each treatment, cell proteins were fractionated by SDS gel electrophoresis and immunoblotted with antibodies against Trx-1 (AbCam), Bcl-2, Mcl-1 (Santa Cruz Biotechnology), ASK-1, phospho-p38, phospho-ERK, phospho-JNK (Cell Signaling) following standard procedures. For NF-κB EMSA, nuclear extracts obtained as described [27], were analyzed using the Gel Shift Assay System (Promega Corporation, Madison, WI) as described [25].

Assay for ASK1-Trx-1 complex formation

The ASK1-Trx-1 complex was immunoprecipitated using Protein A/G PLUS–Agarose beads and following the manufacturer's instructions (Santa Cruz Biotechnology) as described [25].

siRNA silencing of the Trx gene and generation of stable Trx-1 knockdown MCF-7 cells

MCF-7 or MDA-MB231 cells ($0.8X10^5$), were transfected with 100 nM Trx siRNA or control siRNA (Dharmacon) for 72 h using lipofectamine 2000 (Invitrogen). For Trx-1stable knockdown, we used one control and three Trx-1 shRNA SMARTvector 2.0 Lentiviral particles (Thermo Scientific Dharmacon).

$1.5x10^6$ MCF-7 cells at passage 6 were incubated overnight with $4.5x10^5$ titer of lentivirus particles (0.3 MOI/cell) suspended in growth medium with 3 µg/ml polybrene. The infected cells were passaged x3 in selection medium containing 1 µg/mL of puromycin, and assayed for transfection efficiency by immunoblot for Trx-1 and by flow cytometry for endogenous GFP expression. Aliquoted positive cells were stored at -80 ^{o}C. Three Trx-1 knockdown cell lines (C1, C2, and C3) were generated; in all *in vivo* experiments we used cell line C3 and control cells, designated as MCF-$7^{shTrx-1}$ and MCF-$7^{shControl}$, respectively.

In vivo studies

All animal experiments were approved by the Institutional Animal Care and Use Committee (IACUC). 1.5 x 10^6 of breast cancer cells were xenografted subcutaneously in both flanks of 5-6 wk-old female Balb/C nude mice as described [2, 28]. Three days before implanting MCF-7 cells, mice received a 0.72 mg β-estradiol pellet (Innovative Research of America) subcutaneously in their front-back area. Vehicle, P-I or Lipo-P-I administration (once a day, 5d/wk) started when the average tumor volume of MCF-7 xenografts was 160 mm^3 and of MDA-MB231 xenografts was 100 mm^3. *Xenograft growth inhibition* in response to treatment was calculated by comparing the difference in percent increase of tumor growth from their 0 time volume to their volume at sacrifice between drug- and vehicle-treated groups.

Cell death and proliferation in xenografts were determined by TUNEL and Ki-67 immunostaining, as described [29]. COX-2 expression, NF-κB activation and Trx-1 expression were determined by immunohistochemitry (IHC) staining followed standard protocols (Antibodies from Cell Signaling and Abcam, respectively) as reported [29]. *Scoring:* For each slide, 3-5 randomly selected fields (200X) were photographed. For each of these (TUNEL, Ki-67, COX-2, NF-κB and Trx-1), the number of positive cancer cells and the number of all (positive and negative) cancer cells were determined for each photograph by two pathologists blinded to their identity. The average of the results by the two pathologists was then calculated (maximal variation 4.2%).Results were expressed as percent positive cells per tumor.

qPCR of Trx-1 mRNA level from Trx-1 knockdown and control MCF-7 xenografts

Total RNA was isolated using TRIZOL reagent (Invitrogen) from xenografts. The qPCR of Trx-1 mRNA was determined using SYBR Green PCR master mix (A&B Applied Biosystems) in accordance with the manufacture's protocol [30].

Statistical analyses

Results are expressed as Mean±SEM. Differences between groups were determined by the Student's t-test. $p<0.05$ was statistically significant.

Results

P-I inhibits the growth of human breast cancer cells and xenografts

Initially, we determined the growth inhibitory effect of P-I on human breast cancer cell lines representing its major clinical subtypes. The 24-h IC_{50} values of P-I were: *ER* (+): MCF-7 = 79 ± 5.6 μM; *HER2* (+): AU-565 = 198 ± 8.4 μM; and *triple negative*: BT-549 = 127 ± 2.3 μM, MDA-MB231 = 28 ± 2.7 μM, and BT-20 = 89 ± 3.5 μM. We also determined its cytokinetic effect on breast cancer cells and its ability to inhibit the growth of breast cancer xenografts.

P-I decreased the proliferation, blocked the $G_1 \rightarrow S$ cell cycle transition and induced apoptosis in MCF-7 cells (Figure 1A-B). Similar results were obtained with MDA-MB231 cells (Additional file 1). Mice with MDA-MB231 xenografts were treated for 40 days with vehicle or P-I 400 mg/kg/day, starting when the average tumor volume was ~100 mm^3. At the end of the study, the tumor volume of controls was 423±64 mm^3 and of P-I treated mice 157±44 mm^3 ($p<0.01$) (Figure 1C). Therefore, P-I 400 mg/kg/day inhibited the growth of MDA-MB231 xenografts by 266%.

The method of delivery can affect the pharmacological effect of a given drug [31]. For example, doxorubicin in liposomes is more efficacious than free doxorubicin [32, 33]. Such enhanced efficacy is explained by the enhanced permeability and retention ("EPR effect"), which represents the preferential uptake of liposomes by tumor cells due to the "leakiness" of the vessels traversing a tumor [34, 35]. Therefore, we studied the anti-breast cancer effect of P-I formulated in liposomes.

Mice with MCF-7 xenografts were treated for 34 days with P-I 300 mg/kg/day or P-I encapsulated in liposomes (Lipo-P-I) at the same dose or with vehicle, starting when the average tumor volume was ~160 mm^3. Compared to controls, P-I inhibited significantly tumor growth starting on day 29 and continuing until sacrifice, when the tumor volume was 276±23 mm^3 and 195±27 mm^3, respectively ($p<0.05$, Figure 1D). The inhibitory effect of Lipo-P-I became statistically significant starting on day 8 of treatment. At sacrifice, xenografts had regressed compared to baseline, being 14% smaller (137±7 mm^3 vs. 160±9 mm^3; $p=0.09$, significant for trend). Lipo-P-I was more efficacious than P-I ($p<0.05$).

We also determined cell proliferation and cell death in xenografts using Ki-67 staining and the TUNEL assay, respectively (Figure 1C-D). In MDA-MB231 and MCF-7 xenografts, P-I inhibited proliferation ($p<0.05$ and $p<0.05$) and increased apoptosis ($p<0.01$ and $p=0.08$, significant for trend). Both

effects were more pronounced in Lipo-P-I treated animals ($p<0.01$ and $p<0.05$ respectively compared with control).

The effect of P-I on RONS and glutathione levels in MCF-7 and MDA-MB231 cells

RONS are important early mediators of the anticancer effect of modified NSAIDs [36]. Pretreatment of MCF-7 cells with the antioxidant, N-acetyl-cystein (NAC), blocked P-I-induced apoptosis by 70.2% (Figure 2A), indicating that this effect is redox-dependent. Thus we evaluated whether P-I induces RONS in breast cancer cells using the molecular probes DCFDA (detects >10 individual RONS [37, 38]), DHE (detects O_2^-) or MitoSOX Red (specific for mitochondrial O_2^-).

In cell lines, P-I induced concentration-dependently RONS detected by DCFDA, an effect abrogated by pretreating the cells with NAC 15 mM (Figure 3B). O_2^- levels were significantly increased in the entire cell (DHE probe) and even more so in mitochondria (MitoSox Red, Figure 3C). P-I decreased modestly the levels of glutathione (GSH), the major intracellular antioxidant [39], and only at concentrations exceeding its IC_{50} for cell growth (Additional file 2).

The effect of P-I on the eicosanoid pathway

COX-2 is a well-recognized biochemical target of NSAIDs, explaining part of their anti-inflammatory effects. P-I inhibits the production of PGE_2 in NIH3T3 cells, a mouse embryonic fibroblast cell line [2]. Furthermore, COX-2 inhibition by NSAIDs is considered one of the mechanisms by which they prevent cancer [40], although COX-independent effects are well described [41, 42]. We have shown that COX-2 induction results from oxidative stress in cancer cells when treated with NSAID derivatives [41]. However, P-I affected COX-2 expression in vitro in a cell type dependent manner. It suppressed COX-2 expression in MCF-7 cells, while stimulating COX-2 expression and PGE_2 production in MDA-MB231 cells (Figure 2D, Additional file 2). Thus, the change of COX-2 level was independent of RONS in P-I treated breast cancer cells. More importantly, P-I did not significantly change COX-2 expression in xenografts ($p>0.05$, Figure 2E). Therefore, we conclude that the anti-cancer effect of P-I is COX-2 independent.

P-I modulates the thioredoxin system in breast cancer

The thioredoxin system plays a crucial role in maintaining the redox homeostasis of cells by reducing oxidized proteins; such protein oxidation can occur during oxidative stress [43]. In view of the increased RONS levels in response to P-I, we determined the status of Trx-1, the main isoform of Trx, and of TrxR in cultured breast cancer cells, and in their xenografts in mice.

In MCF-7 cells after 1h of treatment, P-I decreased the levels of Trx-1, very modestly at concentrations corresponding to $2xIC_{50}$ and significantly at $3xIC_{50}$. Pretreatment with 15 mM NAC restored the level of Trx-1 , indicating that RONS induction is upstream of Trx-1 (Figure 3A). At $2xIC_{50}$ P-I also promoted the oxidation of Trx-1, with about 1/3 of the protein being oxidized. Similar results were obtained in MDA-MB231 cells (Additional file 3). P-I failed to affect TrxR expression but inhibited its enzymatic activity. In an in vitro assay, which uses purified TrxR from rat liver to assess its ability to reduce an oxidized substrate, DTNB, P-I suppressed the activity of TrxR (IC_{50}= 88 µM). Similarly, the activity of TrxR determined in protein extracts from MCF-7 cells was suppressed following treatment with P-I (Figure 4B).

We examined the expression of Trx-1 in MCF-7 and MDA-MB231 xenografts from the efficacy study mentioned above. IHC staining showed cytosolic and nuclear expression of Trx-1 in both types of tumors (Figure 3C-D). Compared to controls, in MDA-MB231 tumors, P-I decreased Trx-1 expression by 47.4 % (41.5± 8.2 vs. 78.9±12.9, p=0.01). In MCF-7 tumors, free P-I had no significant effect on Trx-1 expression, but Lipo-P-I decreased it by 54.1% (33.3±14 vs. 72.6±7.4, $p<0.05$). Of note, the dose of P-I in animals with MCF-7 xenografts was 300 mg/kg/day and in those with MDA-MB231 tumors was 400 mg/kg/day. This may account for the difference in the inhibition of Trx-1 expression. Although free P-I did not inhibit TrxR activity in either type of xenograft, Lipo-P-I reduced it significantly by 35% in MCF-7 xenografts (p=0.03) (Figure 3C-D).

P-I modulates Trx dependent cell signaling

NF-κB and MAPKs are major determinants of cell renewal and cell death (24, 25). The Trx system is intimately linked to these two signaling pathways. Trx-1 enhances the binding of NF-κB to DNA by reducing the intermolecular Cys62 -S-S- bond of its p50 subunit [12]. Trx-1 controls the activation of

JNK and p38 by binding to ASK1 (26). When Trx-1 is oxidized, ASK1 dissociates from it, autophosphorylates, and activates MAPK cascades. Thus we examined whether the effect of P-I on the Trx system modulates these redox signaling pathways.

P-I inhibited NF-κB activation in MCF-7 cells, whereas 1h pretreatment with 15 mM NAC restored the NF-κB activity to control level (Figure 4A). A similar inhibition was observed in MCF-7 xenografts (Figure 4B). P-I inhibited NF-κB activation by 32% ($p=0.08$ significantly for trend) and Lipo-P-I by 61% ($p<0.05$). Both in vitro and in vivo, P-I suppressed the expression of Bcl-2 and Mcl-1, two anti-apoptotic proteins transcriptionally regulated by NF-κB [44, 45] (Figure 4C). Similar results were found in MDA-MB231 xenografts (Figure 4D).

P-I dissociated the ASK1–Trx-1 complex nearly completely in MCF-7 cells (Figure 5A). Incubation of the cell lysate with the reducing agent DTT restored the complex, indicating that the dissociation of ASK1 from Trx-1 was due to P-I–induced oxidation of Trx-1. We therefore studied the downstream ASK1-MKK4-p38MAPK/JNK signaling. In both cell lines, P-I activated p38 and JNK (it increased their phosphorylation) time- and concentration-dependently. However, P-I suppressed ERK activation, particularly at a high concentration ($2xIC_{50}$). The total levels of these MAPKs were not changed by P-I (Figure 5B). In MCF-7 xenografts, P-I activated JNK and ERK, but not p38. In MDA-MB231 xenografts, P-I activated JNK and p38, but not ERK (Figure 5C). Such differential activation of MAPKs underscores their context-dependence.

Trx-1 mediates the anticancer effect of P-I

To further assess the role of Trx-1 in the anti-breast cancer effect of P-I, we silenced the expression of Trx-1 in breast cancer cells using specific siRNA and determined whether P-I induced cell death was affected. Compared to control cells, the induction of apoptosis by P-I 60 μM or 80 μM was reduced by 91% and 87%, respectively in Trx-1 depleted cells (Figure 6A). Similar results were obtained with MDA-MB231 cells (Additional file 4). As expected [46], there were parallel changes in the levels of O_2^-. P-I failed to induce mitochondrial O_2^- in Trx-1 knock-down cells (Figure 6B).

In vivo, we xenografted nude mice with MCF-$7^{shTrx\text{-}1}$ (Trx-1 stably knocked down) or with MCF-$7^{shControl}$ (control shRNA) cells (Methods and Additional file 5). When the average tumor volume was 162

and 168 mm^3, respectively, animals were treated with P-I 400 mg/kg/day or vehicle. P-I failed to inhibit the growth of MCF-$7^{shTrx-1}$ xenografts during the 24 days of observation. In contrast, compared to the vehicle-treated group, P-I inhibited the growth of MCF-$7^{shControl}$ xenografts by 126% ($p<0.05$) (Figure 6C). The nearly complete suppression of Trx-1 levels in these tumors was confirmed by immunobloting and qPCR (Figure 6D). The effect of P-I on tumor growth reflects its differential cytokinetic effect. Compared to vehicle treated groups, in MCF-$7^{shTrx-1}$ xenografts, P-I failed to alter the rates of apoptosis or proliferation, whereas in MCF-$7^{shControl}$ xenografts, P-I increased apoptosis by 2-fold ($p<0.01$) and suppressed proliferation by 49% ($p<0.05$) (Figure 6E and data not shown).

In these tumors, NF-κB activation showed a similar response to P-I: compared to the vehicle-treated group, there was no statistically significant change in MCF-$7^{shTrx-1}$ xenografts but there was an 80% reduction in xenografts expressing Trx-1 normally ($p<0.03$; Figure 6E). The inactivation of NF-κB by P-I requires the presence of Trx-1. These results strongly support the notion that P-I's anti-breast cancer effect is tightly modulated by Trx-1, the key molecule to turn on the redox signaling.

Discussion

Our results demonstrate that the novel compound P-I is a strong agent against breast cancer, especially when formulated in liposomes, and establish the critical role of the Trx system in mediating this effect through downstream redox signaling.

The effect of P-I against breast cancer is a) broad, encompassing both ER (+) and triple (-) human xenografts; b) strong, as evidenced by the tumor stasis and tumor regression achieved in MDA-MB231 and MCF-7 xenografts respectively; and c) potentially clinically relevant, as these two cell lines represent the most frequent and the most difficult to treat subtypes of breast cancer. Our efficacy study also demonstrated that, in agreement with current understanding [31], formulating P-I in liposomes enhanced its anticancer efficacy.

The anticancer effect of P-I clearly reflects its cytokinetic effect, which consists of inhibition of proliferation and induction of apoptosis, both noted in vitro and in vivo. In keeping with their differential anti-tumor efficacy, liposomal P-I had a more pronounced cytokinetic effect than P-I.

Oxidative stress emerges as a key mechanism of action of several anticancer agents and we have observed it with compounds structurally related to P-I [47, 48]. Indeed, oxidative stress is a very early change that culminates in cell death via apoptosis and necrosis [49]. In the two breast cancer cell lines that we studied, P-I induced oxidative stress, and its inhibition by NAC blocked the effect on cell death.

The thioredoxin system plays a pivotal role in redox homeostasis. P-I had a profound effect on the two protein members of this system, Trx-1 and TrxR. In cultured breast cancer cells, P-I drove Trx-1 towards its oxidized form and reduced the expression of Trx-1 in xenografts. P-I also suppressed the activity of TrxR, determined by an assay using purified enzyme and also in cultured and xenografted breast cancer cells treated with P-I. In contrast to Trx-1, the expression of TrxR was not affected by P-I. Of interest, in MCF-7 xenografts, the more effective Lipo-P-I suppressed Trx-1 expression and TrxR activity more than free P-I, suggesting that this effect may be part of P-I's mechanism of action. These findings substantiate a major suppressive effect of P-I on the thioredoxin system through effects on Trx-1 and TrxR.

The effect of P-I on the thioredoxin system had repercussions on signaling cascades dependent on it, as exemplified by its effects on NF-κB and MAPK. First, the activity of NF-κB was suppressed by P-I in both cultured cells and tumor xenografts. NF-κB is particularly responsive to changes in the Trx system through its Cys62 of p50, whose oxidation renders NF-κB incapable of binding to DNA [12]. The importance of the inactivation of NF-κB following treatment with P-I is indicated by the suppressed expression in xenografts of Bcl-2 and Mcl-1, two anti-apoptotic proteins transcriptionally regulated by NF-κB [44, 45]. The MAPK pathway, also regulated by P-I, is downstream of Trx-1 as well. Trx-1 is normally bound to ASK1, keeping the pathway inactive, but when oxidized, ASK1 is released from the complex activating the downstream MAPK cascade [14]. Of the three main branches of MAPKs, JNK was uniformly activated by P-I in both cell lines and their xenografts. The response of the other two varied in a cell type dependent manner. Clearly, P-I has a context-dependent effect on MAPKs.

While the modulating effect of P-I on these two signaling mechanisms that are downstream of the thioredoxin system is clear, its direct linkage to the thioredoxin system required the study of xenografts with permanently suppressed Trx-1. P-I suppress the activation of NF-κB only when the expression of Trx-1 was intact. Furthermore, its ability to induce apoptosis and suppress proliferation in these xenografts, two effects heavily mediated by NF-κB and MAPK, was abrogated when the expression of Trx-1 was markedly knocked-down by shRNA. Collectively, these data establish the thioredoxin system as an important mediator of the anticancer effect of P-I. Figure 7 outlines the role of P-I in these interactions.

Our findings indicate the role of the thioredoxin system in ensuring cell survival in the face of oxidative stress. As amply demonstrated here, agents like P-I that paralyze this vital control system enhance cell death and inhibit cell proliferation. The final result of any intervention directed at the thioredoxin system likely depends on complex interactions beyond the NF-κB and MAPK cascades. Nevertheless, and in agreement with work by others [4, 20, 50], this system represents an important target for the development of anticancer agents.

Conclusions

Our work establishes P-I as an agent with a strong effect against breast cancer in a preclinical model; suggests that the mode of its delivery may be important for its efficacy; and establish the thioredoxin system as a critical mediator of its mechanism of action. The thioredoxin system, vital for cell homeostasis, emerges as an important target for the development of novel anticancer agents.

Abbreviations

ASK-1: apoptosis signal-regulating kinase 1; Bcl-2: B cell lymphoma 2; COX-2: cyclooxygenase 2; DCFDA: 2',7' –dichlorofluorescein diacetate; DHE: dihydroethidium; DTNB: 5,5′-dithiobis(2-nitrobenzoic acid); DTT: dithiothreitol; EDTA: ethylenedinitrilotetraacetic acid; EMSA: electrophoretic mobility shift assay; ER: estrogen receptor; ERK: extracellular signal-regulated kinase; HER2: human epidermal growth factor receptor-2; IC_{50}: concentration that inhibits cell growth by 50%; IHC: immunohistochemistry; JNK: Jun N-terminal kinase; Lipo-P-I: liposome encapsulated phospho-ibuprofen; MAPK: mitogen-activated protein kinase; Mcl-1: myeloid cell leukemia 1; MTT: methylthiazolyldiphenyl-tetrazolium bromide; NAC: N-acetyl-cysteine; NADPH: nicotinamide adenine dinucleotide phosphate; NF-κB: nuclear factor κB; NSAID: non-steroidal anti-inflammatory drug; PGE_2: prostoglandin E_2; PgR: progesterone receptor; P-I: phospho-ibuprofen; qPCR: quantitative polymerase chain reaction; RONS: reactive oxygen and nitrogen species; shRNA: short hairpin RNA; siRNA: small interfering RNA; Trx-1: thioredoxin 1; TrxR: thioredoxin reductase; TUNEL: terminal deoxynucleotidyl transferase mediated dUTP nick end labeling.

Competing Interests

LR and KV have no competing interests. DK has received compensation from Medicon Pharmaceuticals, Inc. BR has an equity position in Medicon Pharmaceuticals, Inc. BR, LH, GM and YS have filed patent applications related to the study drug. The authors have no non-financial competing interests.

Author's Contribution

YS conceived the study, participated in its design, carried out most of the in vitro and in vivo studies, analysed the data and participated in the preparation of the manuscript. LR performed the western blots and part of immunohistochemistry assays for in vivo studies. LH carried out the in vitro COX-2 expression experiments. GM carried out the NF-κB EMSA assays. KV synthesized batches of P-I. DK participated in study design and data analysis, provided P-I, and reviewed the manuscript. BR conceived the study, participated in its design, supervised the work, analysed data and participated in writing the manuscript. All authors read and approved the final manuscript.

Acknowledgements

Financial support: Grants from the Department of Defense W81XWH1010873 and W81XWH0710187; and from the NIH Grant HHSN261201000109C.

References

1. Jemal A, Bray F, Center MM, Ferlay J, Ward E, Forman D: **Global cancer statistics**. *CA: a cancer journal for clinicians*, **61**:69-90.
2. Huang L, Mackenzie G, Ouyang N, Sun Y, Xie G, Johnson F, Komninou D, Rigas B: **The novel phospho-non-steroidal anti-inflammatory drugs, OXT-328, MDC-22 and MDC-917, inhibit adjuvant-induced arthritis in rats**. *Br J Pharmacol* 2011, **162**:1521-1533.
3. Xie G, Sun Y, Nie T, Mackenzie GG, Huang L, Kopelovich L, Komninou D, Rigas B: **Phospho-Ibuprofen (MDC-917) Is a Novel Agent against Colon Cancer: Efficacy, Metabolism, and Pharmacokinetics in Mouse Models**. *J Pharmacol Exp Ther* 2011, **337**:876-886.
4. Arner ES: **Focus on mammalian thioredoxin reductases--important selenoproteins with versatile functions**. *Biochimica et biophysica acta* 2009, **1790**:495-526.
5. Mukherjee A, Martin SG: **The thioredoxin system: a key target in tumour and endothelial cells**. *Br J Radiol* 2008, **81 Spec No 1**:S57-68.
6. Arner ES, Holmgren A: **The thioredoxin system in cancer-introduction to a thematic volume of Seminars in Cancer Biology**. *Seminars in cancer biology* 2006, **16**:419.
7. Koneru S, Varma Penumathsa S, Thirunavukkarasu M, Vidavalur R, Zhan L, Singal PK, Engelman RM, Das DK, Maulik N: **Sildenafil-mediated neovascularization and protection against myocardial ischaemia reperfusion injury in rats: role of VEGF/angiopoietin-1**. *Journal of cellular and molecular medicine* 2008, **12**:2651-2664.
8. Berndt C, Lillig CH, Holmgren A: **Thioredoxins and glutaredoxins as facilitators of protein folding**. *Biochimica et biophysica acta* 2008, **1783**:641-650.
9. Yoshioka J, Schreiter ER, Lee RT: **Role of thioredoxin in cell growth through interactions with signaling molecules**. *Antioxidants & redox signaling* 2006, **8**:2143-2151.
10. Kaimul AM, Nakamura H, Masutani H, Yodoi J: **Thioredoxin and thioredoxin-binding protein-2 in cancer and metabolic syndrome**. *Free Radic Biol Med* 2007, **43:**861-868.
11. Benz CC, Yau C: **Ageing, oxidative stress and cancer: paradigms in parallax**. *Nature reviews* 2008, **8**:875-879.

12. Matthews JR, Wakasugi N, Virelizier JL, Yodoi J, Hay RT: **Thioredoxin regulates the DNA binding activity of NF-kappa B by reduction of a disulphide bond involving cysteine 62**. *Nucleic acids research* 1992, **20**:3821-3830.

13. Hirota K, Matsui M, Iwata S, Nishiyama A, Mori K, Yodoi J: **AP-1 transcriptional activity is regulated by a direct association between thioredoxin and Ref-1**. *Proceedings of the National Academy of Sciences of the United States of America* 1997, **94**:3633-3638.

14. Saitoh M, Nishitoh H, Fujii M, Takeda K, Tobiume K, Sawada Y, Kawabata M, Miyazono K, Ichijo H: **Mammalian thioredoxin is a direct inhibitor of apoptosis signal-regulating kinase (ASK) 1**. *Embo J* 1998, **17**:2596-2606.

15. Nishinaka Y, Masutani H, Oka S, Matsuo Y, Yamaguchi Y, Nishio K, Ishii Y, Yodoi J: **Importin alpha1 (Rch1) mediates nuclear translocation of thioredoxin-binding protein-2/vitamin D(3)-up-regulated protein 1**. *The Journal of biological chemistry* 2004, **279**:37559-37565.

16. Malhotra JD, Kaufman RJ: **Endoplasmic reticulum stress and oxidative stress: a vicious cycle or a double-edged sword?** *Antioxidants & redox signaling* 2007, **9**:2277-2293.

17. Zhang K: **Integration of ER stress, oxidative stress and the inflammatory response in health and disease**. *International journal of clinical and experimental medicine* 2010, **3**:33-40.

18. Cha MK, Suh KH, Kim IH: **Overexpression of peroxiredoxin I and thioredoxin1 in human breast carcinoma**. *J Exp Clin Cancer Res* 2009, **28**:93.

19. Kim SJ, Miyoshi Y, Taguchi T, Tamaki Y, Nakamura H, Yodoi J, Kato K, Noguchi S: **High thioredoxin expression is associated with resistance to docetaxel in primary breast cancer**. *Clin Cancer Res* 2005, **11**:8425-8430.

20. Powis G, Kirkpatrick DL: **Thioredoxin signaling as a target for cancer therapy**. *Current opinion in pharmacology* 2007, **7**:392-397.

21. Pennington JD, Jacobs KM, Sun L, Bar-Sela G, Mishra M, Gius D: **Thioredoxin and thioredoxin reductase as redox-sensitive molecular targets for cancer therapy**. *Current pharmaceutical design* 2007, **13**:3368-3377.

22. Lacroix M, Leclercq G: **Relevance of breast cancer cell lines as models for breast tumours: an update**. *Breast cancer research and treatment* 2004, **83**:249-289.

23. Huguet EL, McMahon JA, McMahon AP, Bicknell R, Harris AL: **Differential expression of human Wnt genes 2, 3, 4, and 7B in human breast cell lines and normal and disease states of human breast tissue**. *Cancer Res* 1994, **54**:2615-2621.

24. Cailleau R, Young R, Olive M, Reeves WJ, Jr.: **Breast tumor cell lines from pleural effusions**. *J Natl Cancer Inst* 1974, **53**:661-674.

25. Sun Y, Rigas B: **The thioredoxin system mediates redox-induced cell death in human colon cancer cells: implications for the mechanism of action of anticancer agents**. *Cancer research* 2008, **68**:8269-8277.

26. Watson WH, Pohl J, Montfort WR, Stuchlik O, Reed MS, Powis G, Jones DP: **Redox potential of human thioredoxin 1 and identification of a second dithiol/disulfide motif**. *The Journal of biological chemistry* 2003, **278**:33408-33415.

27. Williams JL, Ji P, Ouyang N, Liu X, Rigas B: **NO-donating aspirin inhibits the activation of NF-kappaB in human cancer cell lines and Min mice**. *Carcinogenesis* 2008, **29**:390-397.

28. Mackenzie GG, Sun Y, Huang L, Xie G, Ouyang N, Gupta RC, Johnson F, Komninou D, Kopelovich L, Rigas B: **Phospho-sulindac (OXT-328), a novel sulindac derivative, is safe and effective in colon cancer prevention in mice**. *Gastroenterology* 2010, **139**:1320-1332.

29. Ouyang N, Williams JL, Tsioulias GJ, Gao J, Iatropoulos MJ, Kopelovich L, Kashfi K, Rigas B: **Nitric oxide-donating aspirin prevents pancreatic cancer in a hamster tumor model**. *Cancer Res* 2006, **66**:4503-4511.

30. Gomez E, Gutierrez-Adan A, Diez C, Bermejo-Alvarez P, Munoz M, Rodriguez A, Otero J, Alvarez-Viejo M, Martin D, Carrocera S, Caamaño JN: **Biological differences between in vitro produced bovine embryos and parthenotes**. *Reproduction (Cambridge, England)* 2009, **137**:285-295.

31. Papahadjopoulos D, Allen TM, Gabizon A, Mayhew E, Matthay K, Huang SK, Lee KD, Woodle MC, Lasic DD, Redemann C, Martin FJ: **Sterically stabilized liposomes: improvements in pharmacokinetics and antitumor therapeutic efficacy**. *Proceedings of the National Academy of Sciences of the United States of America* 1991, **88**:11460-11464.

32. Batist G, Harris L, Azarnia N, Lee LW, Daza-Ramirez P: **Improved anti-tumor response rate with decreased cardiotoxicity of non-pegylated liposomal doxorubicin compared with conventional doxorubicin in first-line treatment of metastatic breast cancer in patients who had received prior adjuvant doxorubicin: results of a retrospective analysis**. *Anti-cancer drugs* 2006, **17**:587-595.

33. O'Shaughnessy JA: **Pegylated liposomal doxorubicin in the treatment of breast cancer**. *Clinical breast cancer* 2003, **4**:318-328.

34. Maruyama K: **Intracellular targeting delivery of liposomal drugs to solid tumors based on EPR effects**. *Adv Drug Deliv Rev* 2010, **63**:161-169.

35. Maruyama K, Yuda T, Okamoto A, Kojima S, Suginaka A, Iwatsuru M: **Prolonged circulation time in vivo of large unilamellar liposomes composed of distearoyl phosphatidylcholine and cholesterol containing amphipathic poly(ethylene glycol)**. *Biochimica et biophysica acta* 1992, **1128**:44-49.

36. Sun Y, Huang L, Mackenzie GG, Rigas B: **Oxidative stress mediates through apoptosis the anticancer effect of phospho-NSAIDs: Implications for the role of oxidative stress in the action of anticancer agents**. *The Journal of pharmacology and experimental therapeutics* 2011, **338**:775-83.

37. Bass DA, Parce JW, Dechatelet LR, Szejda P, Seeds MC, Thomas M: **Flow cytometric studies of oxidative product formation by neutrophils: a graded response to membrane stimulation**. *J Immunol* 1983, **130**:1910-1917.

38. LeBel CP, Ischiropoulos H, Bondy SC: **Evaluation of the probe 2',7'-dichlorofluorescin as an indicator of reactive oxygen species formation and oxidative stress**. *Chem Res Toxicol* 1992, **5**:227-231.

39. Forman HJ, Zhang H, Rinna A: **Glutathione: overview of its protective roles, measurement, and biosynthesis**. *Mol Aspects Med* 2009, **30**:1-12.

40. Harris RE: **Cyclooxygenase-2 (cox-2) blockade in the chemoprevention of cancers of the colon, breast, prostate, and lung**. *Inflammopharmacology* 2009, **17**:55-67.

41. Sun Y, Chen J, Rigas B: **Chemopreventive agents induce oxidative stress in cancer cells leading to COX-2 overexpression and COX-2-independent cell death**. *Carcinogenesis* 2009, **30**:93-100.

42. Kashfi K, Rigas B: **Non-COX-2 targets and cancer: expanding the molecular target repertoire of chemoprevention**. *Biochemical pharmacology* 2005, **70**:969-986.

43. Circu ML, Aw TY: **Reactive oxygen species, cellular redox systems, and apoptosis**. *Free radical biology & medicine* 2010, **48**:749-762.

44. Tamatani M, Che YH, Matsuzaki H, Ogawa S, Okado H, Miyake S, Mizuno T, Tohyama M: **Tumor necrosis factor induces Bcl-2 and Bcl-x expression through NFkappaB activation in primary hippocampal neurons**. *The Journal of biological chemistry* 1999, **274**:8531-8538.

45. Mitsiades CS, Mitsiades N, Poulaki V, Schlossman R, Akiyama M, Chauhan D, Hideshima T, Treon SP, Munshi NC, Richardson PG, Anderson KC: **Activation of NF-kappaB and upregulation of intracellular anti-apoptotic proteins via the IGF-1/Akt signaling in human multiple myeloma cells: therapeutic implications**. *Oncogene* 2002, **21**:5673-5683.

46. Rigas B, Sun Y: **Induction of oxidative stress as a mechanism of action of chemopreventive agents against cancer**. *Br J Cancer* 2008, **98**:1157-1160.

47. Sun Y, Rigas B: **The Thioredoxin System Mediates Redox-Induced Cell Death in Human Colon Cancer Cells: Implications for the Mechanism of Action of Anticancer Agents**. *Cancer Res* 2008, **68**:8269-8277.

48. Huang L, Mackenzie G, Ouyang N, Sun Y, Xie G, Johnson F, Komninou D, Rigas B: **The novel phospho-NSAIDs OXT-328, MDC-22 and MDC-917 inhibit adjuvant-induced arthritis in the rat.** *Br J Pharmacol* 2011, **162**:1521-33.

49. Orrenius S, Gogvadze V, Zhivotovsky B: **Mitochondrial oxidative stress: implications for cell death**. *Annual review of pharmacology and toxicology* 2007, **47**:143-183.

50. Holmgren A, Lu J: **Thioredoxin and thioredoxin reductase: current research with special reference to human disease**. *Biochemical and biophysical research communications* 2010, **396**:120-124.

Figure legends

Figure 1. P-I inhibited the growth of breast cancer cells and xenografts.

(**A**) Proliferation (BrdU/propidium iodide staining; *upper panel*) and cell cycle (propidium iodide staining, *lower panel*) of MCF-7 cells treated with P-I was evaluated by flow cytometry and results were quantified (*right panel*). (**B**) Apoptosis of MCF-7 cells treated with P-I was evaluated by annexin V and propidium iodide staining. Tumor growth curve of MDA-MB231 xenografts (treated with P-I 400 mg/kg/day or vehicle) (**C**) and MCF-7xenografts (treated with P-I 300 mg/kg/day, Lipo-P-I at the same dose, or vehicle) (**D**) are shown. Quantification of cell proliferation (Ki67) or cell death (TUNEL) staining are shown on the right of their representative images (200 x magnifications) as indicated.

Figure 2. Effect of P-I on RONS and COX-2 levels in breast cancer.

(**A**) Pretreating MCF-7 cells with NAC 15mM suppressed P-I-induced apoptosis. (**B**) After 1h treatment, MCF-7 cells as indicated were stained with DCFDA and fluorescent intensity was determined by flow cytometry. (**C**) *Left*: After 1h treatment with P-I 1.5xIC_{50}, MCF-7 cells were stained with MitoSOX Red or DHE and fluorescent intensity was determined by flow cytometry. *Right:* Confocal microscopy of MitoSOX Red stained MCF-7 cells after same treatment as above. *Upper panel*: MitoSOX Red alone. *Lower panel*: MitoSOX Red merged with DIC images. (**D**) COX-2 levels in MDA-MB231 cells were detected by immunoblot; loading control: β-actin. After a 6 h-treatment with P-I, PGE_2 levels were assayed in the culture medium of MDA-MB231 cells using a kit from Cayman Chemicals. Results are folds over control. (**E**) Representative images (200X magnification) from IHC stained COX-2 in MDA-MB231 xenografts (those in Figure 1C) and their quantification are shown. Insets: The 600X images of COX-2(+) cells.

Figure 3. Effect of P-I on the thioredoxin system in breast cancer.

(**A**) *Upper panel*: Trx-1 levels in MCF-7 cell lysates were determined by immunoblot. *Lower panel:* The redox status of Trx-1 in MCF-7 cells was assayed as in Methods after 1h treatment with P-I. ox= oxidized form, red= reduced form of Trx-1. (**B**) P-I reduces TrxR activity. The effect of P-I on the enzymatic activity of TrxR was assayed in vitro using TrxR purified from rat liver (*left*). The TrxR activity was determined in

protein extracts from MCF-7 cells treated with P-I for 1h (*right*). Representative images (200X magnification) of Trx-1 in MCF-7 (**C**) or MDA-MB231 (**D**) xenografts by IHC staining and quantifications are shown. (**E**) TrxR activity was determined in MCF-7 tumor lysates.

Figure 4. P-I inhibited NF-κB signaling in breast cancers.

(**A**) *Left panels*: NF-κB-DNA binding was determined by EMSA in nuclear fractions of MCF-7 cells treated with or without P-I. 0: Control nuclear fraction incubated with 100-fold molar excess of specific (+S) or non-specific (+NS) unlabeled oligonucleotide containing the consensus sequence of NF-κB. *Right panels*: Immunoblots of Bcl-2 and Mcl-1 from MCF-7 cells treated with or without P-I as indicated. Representative images (200X) of IHC staining of activated NF-κB in MCF-7 (**B**) and MDA-MB-231 (**D**) xenografts (as in Figure 1) and quantification results are shown. Immunoblots of Bcl-2 and Mcl-1 from the lysates of MCF-7 (**C**) and MDA-MB231 xenografts (**D**, as indicated) are shown. #, $p<0.05$; *, $p<0.001$. Loading control: β-actin.

Figure 5. P-I modulated MAPKs in breast cancers.

(**A**) P-I dissociates ASK1-Trx-1 complex in MCF-7 cells. Total cell lysates from vehicle or P-I treated cells were immunoprecipitated using anti-Trx-1 antibody in the presence (+) or absence (-) of DTT. Supernatants (IB) and immunoprecipitants (IP) were immunoblotted with anti-ASK1 and anti-Trx-1, respectively. (**B**) MAPKs activity was determined by immunoblotting MCF-7 cell lysates with antibodies against phosphorylated or total MAPKs as indicated. (**C**) Effect of P-I on MAPK signaling in breast cancer xenografts. Protein lysates from MCF-7 xenografts (*upper*) or from MDA-MB231 xenografts (*lower*) as described in Figure 1 were immunoblotted with antibodies against phosphorylated MAPKs. Loading control: β-actin. Results were quantified and graphed on the right. #, $p<0.05$; *, $p<0.001$.

Figure 6. Trx-1 mediates the anticancer effect of P-I in vitro and in vivo.

(**A**) MCF-7 cells transfected with Trx-1 siRNA (TrxsiRNA) or control siRNA (CtlsiRNA) for 72 h were treated with P-I for 16 h. Cell death was assayed after annexin V staining. Immunoblots on the right shows the Trx-1 level in these cells. (**B**) Transient transfected MCF-7 cells were assayed for

mitochondrial O^{2-} after treatment with P-I for 1h. (**C**) Permanent Trx-1 knockdown (MCF-$7^{shTrx-1}$) and its control (MCF-$7^{shControl}$) cells were xenografted into nude mice, which treated with P-I or vehicle. Tumor growth curves are shown. (**D**) At end point, Trx-1 expression in vehicle treated tumors was determined by immunoblot for protein level or qPCR for mRNA level. (**E**) Cell death (TUNEL) and active NF-κB xenografts as above were determined by IHC. Representative images (200X) from each group and quantification results are shown as indicated.

Figure 7. Effect of P-I against breast cancer: Proposed mechanism of action.

In this model, P-I suppresses breast cancer growth through its dual effect a) on RONS, inducing oxidative stress; and b) on the Trx system, inhibiting the TrxR activity, oxidizing Trx-1 and suppressing its expression. These effects lead to decreased cell proliferation and increased apoptosis, their net result suppressed breast cancer growth or even tumor regression. Specifically, P-I-induced RONS convert proteins from their reduced (Protein-*red*) to oxidized (Protein-*ox*) state. Trx-1, Trx-1-$(SH)_2$, reduces its oxidized client proteins, being, however, itself oxidized in the process (Trx-1-S_2). TrxR recycles Trx-1-S_2 back to its normal reduced state. The shaded areas explain how the effect of P-I on redox signalings (NF-κB and ASK-1-p38/JNK) is controlled by the central Trx system.

Additional file

Additional file 1. Cell kinetic effect of P-I in MDA-MB231 cells

Cell death (**A**) and proliferation (**B**) were examined by Annexin V/PI staining or BrdU staining, respectively, after MDA-MB231 cells were treated with or without P-I for 16 hs.

Additional file 2. P-I affect redox status and COX-2 in breast cancer cells.

(**A**) MDA-MB231 cells treated with P-I for 1 h were stained with DCFDA and their fluorescent intensity was determined by flow cytometry. (**B**) GSH content of MDA-MB231 cells treated with P-I for 3 h was determined in cell lysates (*: $p<0.01$). (**C**) COX-2 was determined by immunoblot in MCF-7 cells treated with P-I.

Additional file 3. P-I oxidized Trx-1 in MDA-MB231 cells

The redox status of Trx-1 in MDA-MB231 cells treated with P-I for 1 h was determined as in Methods. ox = oxidized form; red = reduced form.

Additional file 4. Trx-1 modulates P-I-induced cell death in MDA-MB231 cells

MDA-MB231 cells were transfected with Trx-1 or control siRNA for 72 h and then treated with P-I for 16 h. Cell death was evaluated by annexin V staining. P-I-induced cell death is shown as % of annexin V(+) cells over control (*: $p<0.01$).

Additional file 5. GFP level in stable Trx-1 knockdown MCF-7 cells

MCF-7 cells were stably transfected with three Trx shRNA (Trx-C1, Trx-C2 and Trx-C3) or control shRNA in SMART vectors containing GFP. The transfection efficiency was determined by comparing the levels of Trx-1 protein (western blot, *upper panel*) or endogenous GFP (flow cytometry, *lower panel*) in stable cell lines with the wild type (WT) cell line.

Figure 1

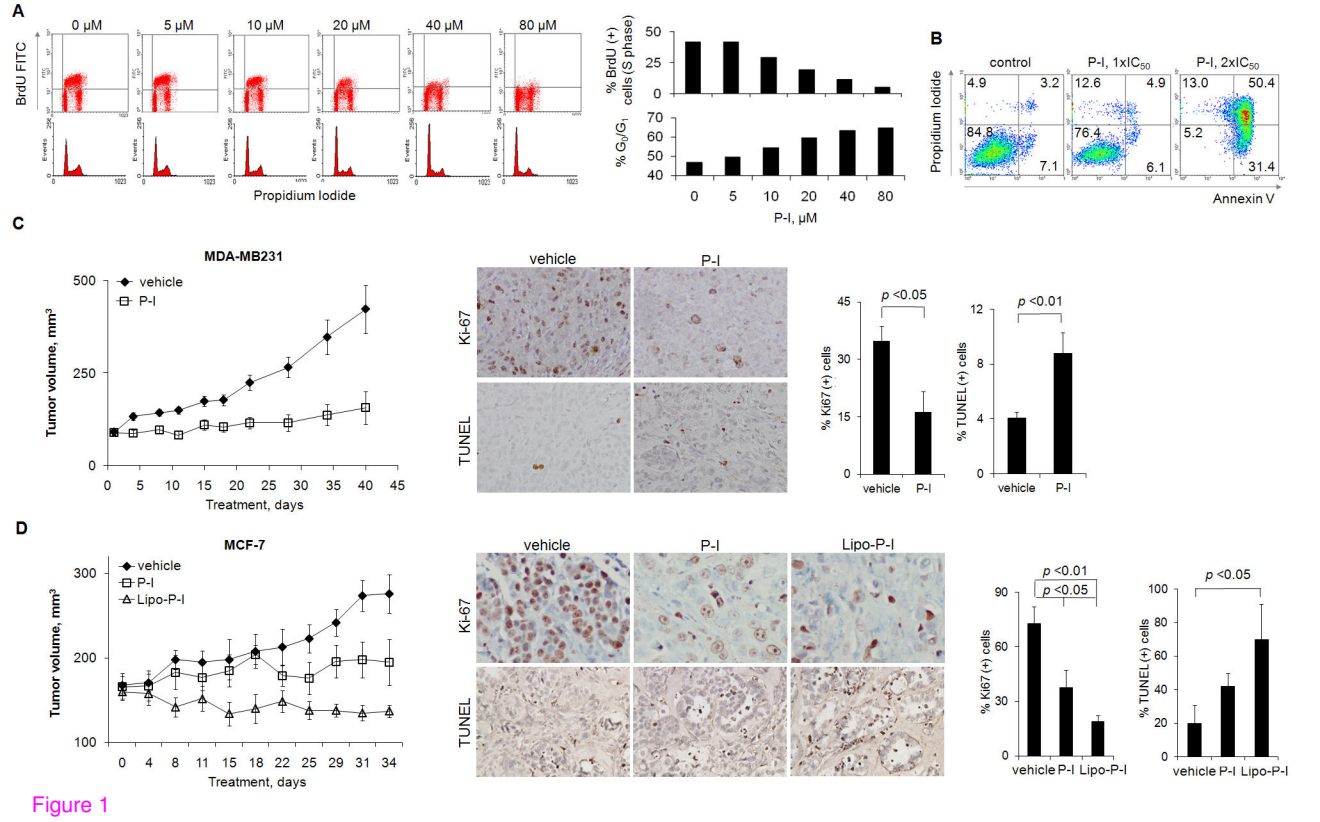

Figure 1

Figure 2

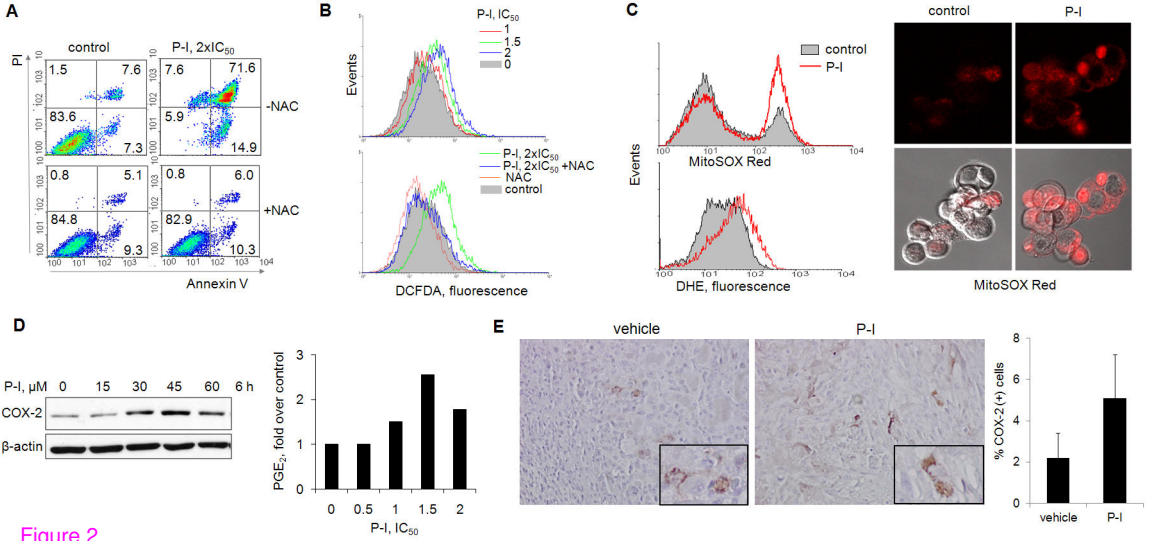

Figure 2

Figure 3

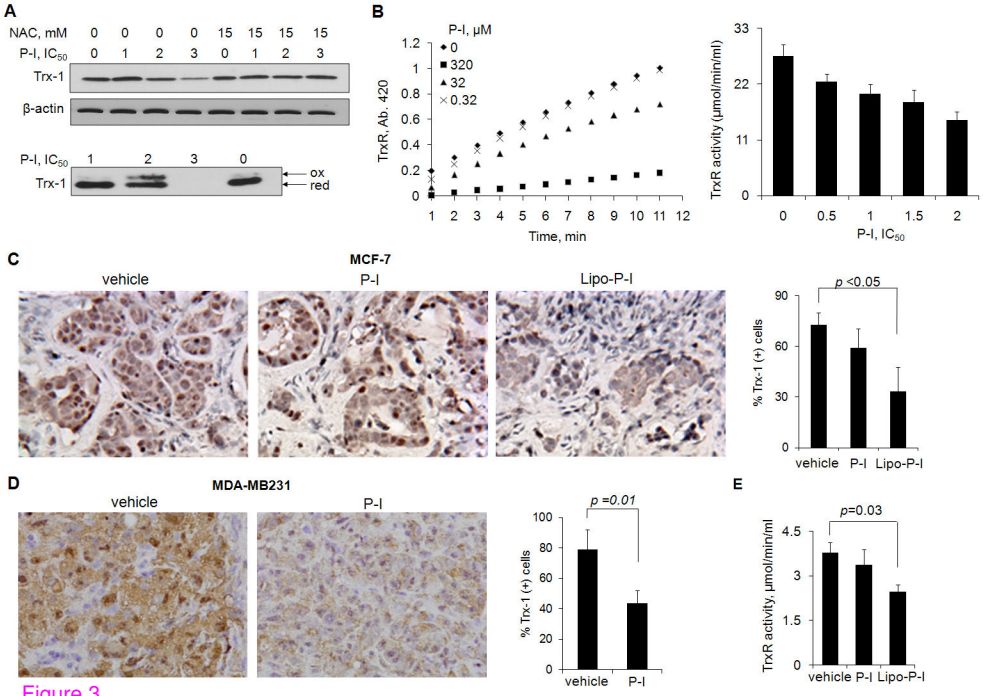

Figure 3

Figure 4

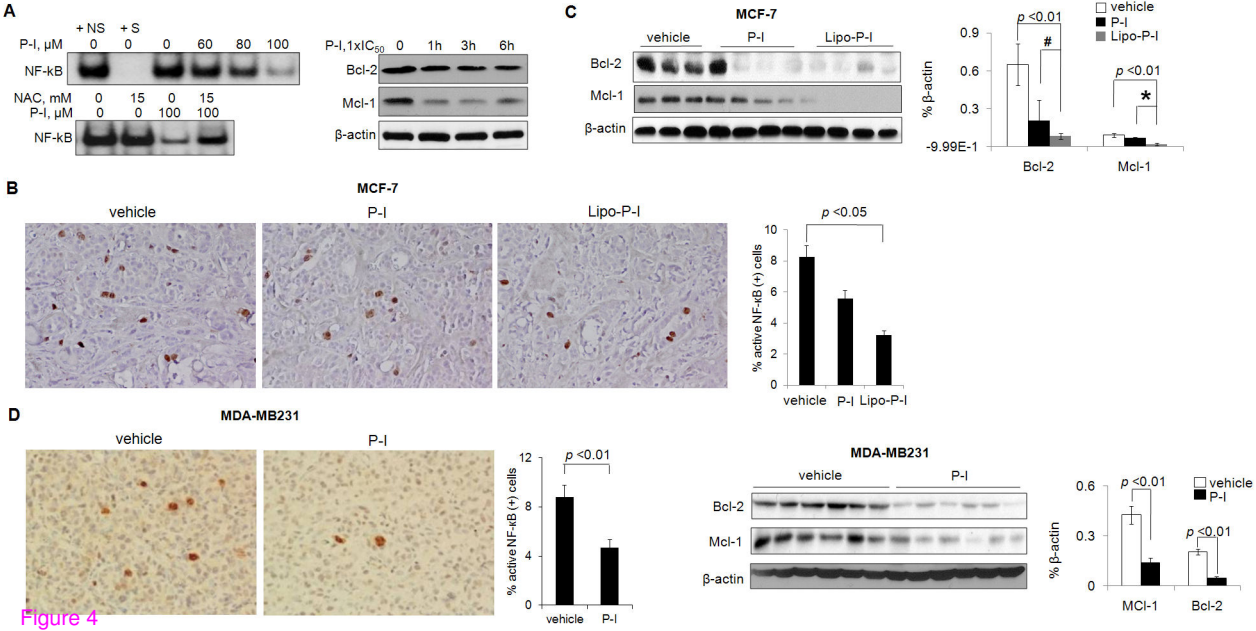

Figure 4

Figure 5

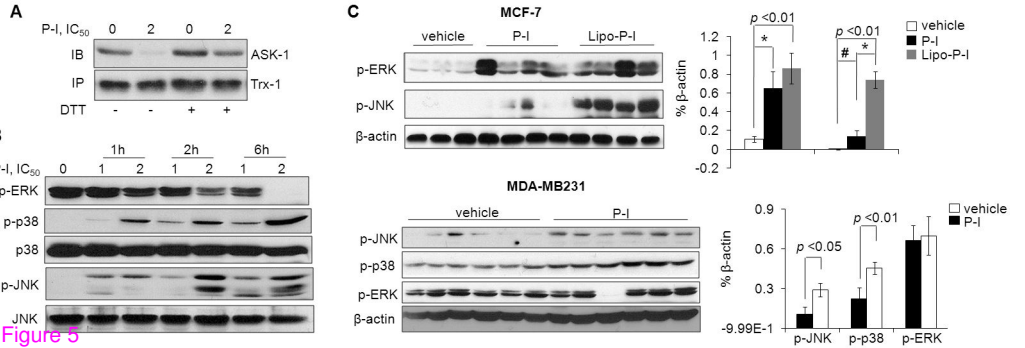

Figure 5

Figure 6

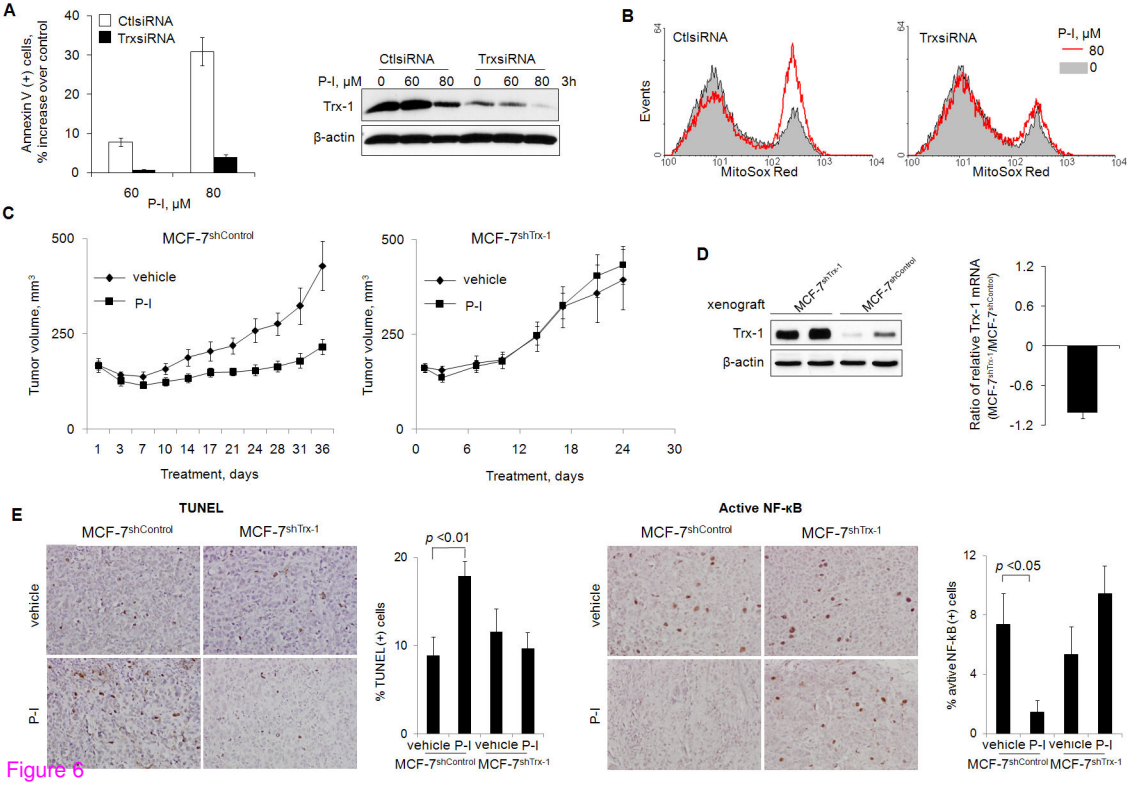

Figure 6

Figure 7

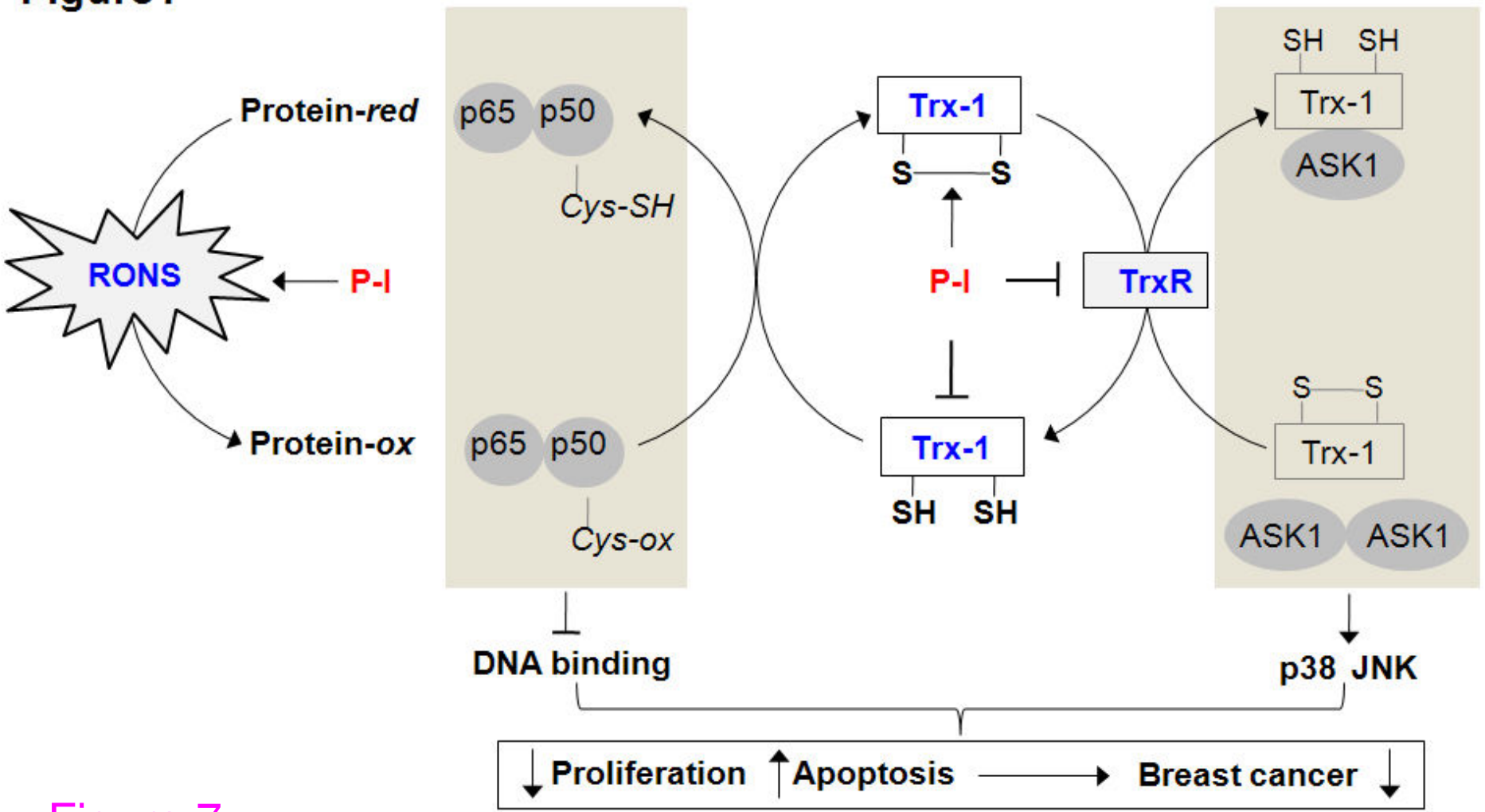

Figure 7

Additional files provided with this submission:

Additional file 1: Addtional file 1.tif, 5522K
http://breast-cancer-research.com/imedia/1266027250670190/supp1.tiff
Additional file 2: Addtional file 2.tif, 12141K
http://breast-cancer-research.com/imedia/1456528310670190/supp2.tiff
Additional file 3: Addtional file 3.tif, 2902K
http://breast-cancer-research.com/imedia/9273494716701909/supp3.tiff
Additional file 4: Addtional file 4.tif, 4302K
http://breast-cancer-research.com/imedia/1335892022670190/supp4.tiff
Additional file 5: Addtional file 5.tif, 14903K
http://breast-cancer-research.com/imedia/7411111856701903/supp5.tiff